STUDY OF DIESEL ENGINE PERFORMANCE AND EMISSIONS DURING A TRANSIENT CYCLE APPLYING AN ENGINE MAPPING-BASED METHODOLOGY

E.G. Giakoumis*, A.I. Alafouzos

Internal Combustion Engines Laboratory, Thermal Engineering Department,
School of Mechanical Engineering, National Technical University of Athens,
9 Heroon Polytechniou St., Zografou Campus, 15780, Athens, Greece

Abstract

An engine mapping-based methodology was developed in order to be able to make a first approximation of the engine performance and emissions during a speed/torque vs. time Transient Cycle. The procedure is based on a previous steady-state experimental investigation of the engine for the formulation of polynomial expressions of all interesting engine properties with respect to engine speed and torque. Correction coefficients are then applied to account for transient discrepancies based on individual transient experiments. The developed algorithm was applied for the case of a heavy-duty diesel engine running on the European Transient Cycle. A comparative analysis was performed for each section of the Cycle, which revealed that the first part (urban driving) is responsible for the biggest amount of emissions (in g) owing to the most frequent and abrupt load changes involved. The obvious advantage of the proposed methodology is the fact that the effect of internal or external (after-treatment) measures can be easily incorporated in the code and quantified in terms of emissions improvement.

Keywords: Diesel engine; Transient operation; Nitric oxide; Soot; Fuel consumption; European Transient Cycle

* Corresponding author. Tel.: +30 210 772 1360, Fax: +30 210 772 1343.
E-mail address: vgiakms@central.ntua.gr (E.G. Giakoumis)

1. Introduction

The turbocharged diesel engine is nowadays the most preferred prime mover in medium and medium-large units applications (truck driving, land traction, ship propulsion, electrical generation). Moreover, it continuously increases its share in the highly competitive automotive market owing to its reliability that is combined with overall very good fuel efficiency. Particularly its transient operation is of great importance in the everyday operating conditions of engines, being often linked with off-design (turbocharger lag) and consequently non-optimum performance; the latter is realized as slow response as well as overshoot in particulate, gaseous and noise emissions. Acknowledging these facts, various legislative Directives in the European Union, Japan and the US, have drawn the attention of automotive manufacturers and researchers all over the world to the transient operation of (diesel) engines, in the form of Transient Cycles Certification for new vehicles [1,2]. A Transient Cycle is usually characterized by long duration (up to 30 minutes) consisting of both speed and load changes under varying operating schedules simulating real driving conditions.

During the last decades, the modeling and the experimental investigation of the thermodynamic and gas dynamic processes in diesel engines has intensively supported the study of engine transient operation [3-10]. However, the vital issue of exhaust emissions as well as the overall engine and vehicle performance during a Transient Cycle – although of primary concern to engine manufacturers – has not been investigated adequately but rather segmentally owing to the following two major issues:

a) As regards the modeling approach, incorporation of exhaust emission predictions into transient (filling and emptying) simulation codes, via two- or better still multi-zone models, would lead to high or even prohibitive computational times for the thousands of engine cycles needed to be simulated during a Transient Cycle.
b) As regards the experimental approach, Transient Cycles require highly complicated, sophisticated and costly experimental facilities (a fully automated test-bed with electronically controlled motoring and dissipating dynamometer, fast response exhaust gas analyzers, dilution tunnels, *etc*.) to be accurately reproduced such as the Constant Volume Sampling system; this fact has limited the availability of transient experimental investigations and results primarily to individual load acceptance or speed accelerations of the order of a few seconds rather than investigation of the engine performance during the whole Transient Cycle [6].

The aim of this paper is to fill an apparent gap in the literature by applying a fast and, relatively easy in terms of cost and laboratory reproduction, evaluation of the performance and emissions (for the present study, these include NO and soot) of a heavy-duty diesel engine during a Transient Cycle. The approach, which lies between simulation and experiment, is based on quasi-steady experimental mapping of the engine in hand applying suitable correction coefficients to account for transient discrepancies; the latter are derived from individual transient experiments (load and speed increases) such as the ones experienced during the Cycle. By so doing, the above-mentioned obstacles for the reproduction of a Transient Cycle, i.e., extremely high computational time or costly and sophisticated experimental facilities can be overcome. Similar engine mapping-based approaches have been developed in the past following in general the context of quasi-linear modeling. For example, Berglund [11] used tabulated data of brake torque vs. speed and fueling, derived at steady-state conditions for vehicular acceleration and load acceptance transients. Rackmil et al. [12] followed the same approach for load and speed increase transients and also applied a correction coefficient to account for transient discrepancies based on an earlier phenomenological simulation code. Nonetheless, as far as the authors are concerned, none of these earlier approaches has ever been employed for the analysis of engine performance during a Transient Cycle. The developed algorithm is applied to a diesel engine running on the European Transient Cycle used for the certification of heavy-duty diesel engines in the European Union but can be easily employed to any other torque/speed vs. time transient schedule.

2. European Transient Cycle (ETC)

The European Transient Cycle (ETC) has been introduced for emission certification of heavy-duty diesel engines in Europe starting in the year 2000 (EC Directive 1999/96/EC) [13]. Different driving conditions are represented by three parts (each of 600 s duration) of the Cycle, incorporating urban (first part), rural (second part) and motorway (third part) driving as well as motoring sections. Figure 1 illustrates normalized engine speed and normalized engine torque vs. time for the ETC Cycle; for the specific engine under test, speed is de-normalized using the following equation [13]

$$\text{Actual Speed} = \frac{\%\ \text{speed}\ (\text{reference speed} - \text{idle speed})}{100} + \text{idle speed} \tag{1}$$

with the reference speed N_{ref} corresponding to the 100% speed values specified in the engine dynamometer schedule, defined as follows:

$$N_{ref} = N_{lo} + 95\%\left(N_{hi} - N_{lo}\right) \tag{2}$$

with N_{hi} the highest engine speed, where 70% of the declared (by the manufacturer) maximum power occurs, and N_{lo} the lowest engine speed, where 50% of the declared maximum power occurs.

Similarly, engine torque is de-normalized to the maximum torque at the respective rotational speed using the following equation:

$$\text{Actual Torque} = \frac{\%\ \text{torque} \cdot (\text{max.torque})}{100} \tag{3}$$

with the maximum torque value found from the respective engine mapping curve.

3. Simulation

3.1 General procedure

For the estimation of the performance and emissions during the Transient Cycle, the procedure illustrated schematically in Fig. 2 is followed. A detailed experimental investigation of the engine in hand is initially undertaken for the (quasi-steady) mapping of the engine operation; the more the discrete engine speed points taken into account the better it is for the accomplishment of the engine mapping. It is important that measurements at very low engine loads are available for a more accurate formulation of engine mapping, since as will be discussed later, various load changes in the Cycle commence from a very low or even zero loading. For each engine rotational speed, a 3rd or 4th order polynomial is formulated for every interesting property with respect to engine torque (recall that a heavy-duty engine Transient Cycle is expressed in terms of engine speed and torque vs. time). For the current investigation, the engine properties under consideration are nitric oxide (NO), soot, fueling (hence carbon dioxide emissions) and power, although any other property (e.g. NO_x, CO, HC, particulates, noise etc) can be easily formulated with the above-mentioned procedure. NO and soot emissions were chosen for the present analysis owing to the fact that a detailed set of experimental measurements for these two pollutants was available for the engine under study under both steady-state and transient conditions. In the analysis that follows, it is not, by any means, implied that the NO or soot values computed should be used as surrogates for the legislated NO_x and particulate matter. Particularly as regards NO, the corrections required by the legislation [13] have been carried out in order to convert the obtained steady-state values on a wet/dry basis.

The upper sub-diagram of Fig. 3 demonstrates the obtained results for the mapping of NO, soot and fueling for the current engine under study over the whole speed and load (torque) operating range. Moreover, the lower sub-diagram of Figure 3 illustrates, in more detail, the emission results for the 1000 rpm operation. The main technical characteristics of the engine under study are given in Table 1. For each Transient Cycle operating point, i.e., at each ‘second’ of the Cycle, a linear interpolation is performed in order to calculate the actual quasi-steady emissions for the particular (de-normalized) engine rotational speed and torque before applying correction factors to account for transient discrepancies; artificial neural network technique could be applied too [14,15].

3.2 Transient discrepancies

As it has long been established, turbocharger lag is the most notable off-design feature of diesel engine transient operation that significantly differentiates the torque pattern from the respective steady-steady conditions. It is caused because, although the fuel pump responds rapidly to the increased fueling demand after a load or speed increase, the turbocharger compressor air-supply cannot match this higher fuel-flow instantly, but only after a number of engine cycles owing to the inertia of the whole system. As a result of this slow reaction, the relative air–fuel ratio during the early cycles of a transient event assumes very low values, deteriorating combustion and leading to slow engine response, long recovery period and overshoot in particulate, gaseous and noise emissions. The above described phenomena, which are more serious the lower the initial load or speed of the individual transient event, are experienced continuously during a Transient Cycle (see also Table 3 later in the text).

In order to account for the above-mentioned serious transient discrepancies but at the same time not deviate from the initial goal of a simple and fast algorithm, correction coefficients were applied to the quasi-steady emissions of Fig. 3, based on various experimental results at transient conditions obtained at the authors’ laboratory on the particular engine. In a previous paper by Ericson et al. [16], the correction coefficients applied were based on air-fuel ratio variations during transients; in the present work, a different procedure was followed influenced by the following, rather unique, characteristic of the engine in hand.

Owing to the narrow speed range of the engine (1000–1500 rpm), the actual engine rotational speed deviation during the whole Transient Cycle is very short (cf. lower sub-diagram of Fig. 5 later in the text), the absolute engine speeds are all very low (engine speed ranges from 800–1027 rpm), and, mainly, the respective accelerations are almost insignificant (cf. Table 3 later in the text – maximum acceleration is 10.52% at t=21 s, and mean acceleration 'only' 2.81% during the Cycle). Hence, for the current engine, it is *only* the load changes that actually contribute to the transient emissions increase during the ETC. Moreover, since all the load steps during the Cycle commence from relatively low initial engine speeds, the well-known fact that load changes commencing from high speeds are less severe than the ones commencing from lower engine speeds (owing to higher initial turbocharger boost pressure) need not be taken into account. The transient emissions correction procedure was based on the following two well-established facts [6]:

a) the transient emission overshoot is higher the greater the load increase (change);

b) the transient emission overshoot is higher the lower the initial load (hence the smaller the initial turbocharger boost pressure, which results in a harder turbocharger lag period).

In order to assess the emission overshoot experienced by the engine during transients compared with the respective quasi-steady conditions, various individual load increases, such as the ones experienced during the ETC, were conducted and analyzed at the authors' laboratory on the engine under study. Elaboration of these experimental transient emission results revealed that, for the current engine configuration, the transient emissions increase could be very effectively accounted for by applying the following 'simple' equation (which incorporates the effect of point 'a' mentioned above)

$$\begin{aligned}&\text{Transient Emissions}(t) = \text{Steady-steady Emissions}(t)\times \\ &\times\left\{1 + c\cdot\left(\text{relative load-increase}\right)_{t-1}^{t}\times\left(\text{speed change}\right)_{t-1}^{t}\right\}\end{aligned} \tag{4a}$$

However, owing to the fact that many load changes during the ETC commence from zero initial loading, Eq. (4a) is transformed into

$$\begin{aligned}&\text{Transient Emissions}(t) = \text{Steady-steady Emissions}(t)\times \\ &\times\left\{1 + c_{\text{load}}\cdot\left(\frac{(\text{current load change})_{t-1}^{t}}{\text{maximum load change}\,(0\% \rightarrow 100\%)}\right)\right\}\times\left(\text{speed change}\right)_{t-1}^{t}\end{aligned} \tag{4b}$$

In other words, correction coefficient c_{load} (different values for soot and NO) increases the instantaneous quasi-steady emissions at each operating point (second) in the Cycle based on the load (and speed) increase encountered from the previous to the current operating point (second).

Obviously, the c_{load} coefficient cannot be assumed constant throughout the whole engine operating range. In order to estimate its value (and at the same time incorporate the effect of the above-mentioned point ‘b’ in our analysis) we divided the various possible load increases into four regimes. The first regime comprises the load increases commencing from a very low initial load (0–20%). This is the most difficult case for the engine since the turbocharger operates at or near zero boost pressure and the turbocharger lag is most prominent during the transient event. The second regime comprises the load increases commencing from an initial load of 21–40%, the third regime comprises the load increases commencing from an initial load of 41–60%, and the fourth those commencing from an initial load higher than 60%, where the turbocharger lag effects are milder, consequently the value of the c_{load} coefficient smaller. Hence, we have derived four values of coefficient c_{load} for soot emissions and four values for NO emissions (with the soot constant found to have a value roughly one order of magnitude higher than its NO counterpart), depending, each time, on the initial load of the transient load increase.

Obviously, the last term at the right-hand side of Eqs (4), i.e. the speed-change term, serves as a further (small) correction factor; as was mentioned earlier, no detailed speed change effects were investigated experimentally owing to the negligible speed increases during the ETC for the current engine.

The following two assumptions are also valid for the analysis that follows: a) during the motoring segments of the Cycle, fueling as well as NO and soot emissions are zero; and b) cold start emissions are ignored – instead the engine is assumed to be in fully warmed-up conditions from the beginning of the Cycle. Ignoring the cold start emissions may, in general, influence instantaneous and total emission results but this holds particularly true for the CO and HC emissions which are not considered in this study. On the other hand, NO (and NO_x) emissions during cold starting are very small owing to the low gas temperatures involved, and may actually be overestimated by the present methodology, when ignoring the lower temperatures encountered right after cold starting.

4. Results and discussion

Application of the simulation procedure described in the previous section (based on the flowchart depicted in Fig. 2) is demonstrated in Figs 4 and 5 for a turbocharged and aftercooled diesel engine without any after-treatment. Figure 4 illustrates the engine performance during the ETC Transient Cycle with Fig. 5 focusing on the instantaneous and cumulative exhaust emissions. Notice the strong influence of instantaneous torque on the performance results in Fig. 4 as well as the practically constant engine speed during the motorway section, partially owing to the rather narrow speed range of the engine in hand. The points where the most abrupt load increases are experienced lead also to a considerable overshoot in emissions that is why a 'broken' y-axis was chosen for the depiction of soot in Fig. 5.

Net soot production (fueling as well, hence CO_2 emissions) is mainly dependent on engine load. As the load increases, more fuel is injected into the cylinders, increasing the temperatures in the fuel-rich zones. Moreover, the duration of diffusion combustion is increased favoring soot formation, whereas the remaining time after combustion as well as the availability of oxygen – both of which enhance the soot oxidation process – decrease; thus, the production of soot is favored.

During the transient load or speed increases of the Cycle, the above mechanism is remarkably enhanced by the locally very high values of fuel–air ratios experienced during turbocharger lag. For the overshoot in soot emissions observed therefore in Fig. 5 after each load or speed increase, the main cause is the instantaneous lack of air due to turbocharger lag, aided by the initial sharp increase in ignition delay during the early transient cycles of each individual load acceptance or acceleration. Rapid increases in fuel injection pressure upon the onset of each instantaneous load step increase cause the penetration of the liquid fuel jet within the combustion chamber to increase [6]. Since the initial higher-pressure fuel jets are injected into an air environment that is practically unchanged from the previous steady-state conditions, the higher-momentum fuel jet is not accompanied by equally enhanced gas motion. Liquid fuel impingement on the cool combustion walls increases, lowering the rate of mixture preparation and enhancing the heterogeneity of the mixture. Moreover, the subsequent harder combustion course prolongs combustion and reduces the available time for soot oxidation [6,7].

For NO emissions, it is, again, the lag between increased fueling and the response of the air-charging system that is responsible for the overshoot in emissions (in engines equipped with exhaust gas recirculation, the EGR starvation during the first cycles of a load increase or acceleration transient event enhances the above trend). Since the main parameter affecting NO formation is the burned gas temperature, local high temperatures due to close to stoichiometric air–fuel mixtures increase NO emissions during the turbocharger lag cycles. Another primary mechanism that affects NO formation is the in-cylinder oxygen availability. Following the rapid decrease in the air–fuel ratio, oxygen concentration is rather limited during the turbocharger lag cycles.

The fueling curve in Fig. 4 corresponds to carbon dioxide (CO_2) emissions too. As a *first approximation,* assuming complete combustion, 1 kg/h of diesel fuel generates approximately 3.106 kg/h CO_2. Of course, owing to the instantaneous lack of air during the early cycles after each transient in the Cycle, the above relation between CO_2 and fueling is not always valid (CO is produced at the expense of CO_2) eventually leading to overestimated carbon dioxide emissions (that is why these emissions are not analyzed in detail in the text but are only illustrated in Fig. 5 for comparative purposes).

Integration of the instantaneous values over the 1800 s of the Cycle yields the total emissions. For the integration, the following formula is applied according to the current European regulations [13]

$$\text{Cumulative Emission} = \frac{\sum_{t=1}^{1800s} \text{Emission}(t)}{\sum_{t=1}^{1800s} \text{Work}(t)} \tag{5}$$

Figure 6 expands on the results of Figs 5 and 6 by detailing the cumulative emissions in the three sections of the Cycle. Clearly, the first part (urban driving) is responsible for the biggest contribution of emissions (in g), particularly soot, which is primarily influenced by abrupt transients. The main characteristics of urban driving that are responsible for the increased amount of soot emissions during this section are summarized below (see also Tables 2 and 3 that detail various (transient) characteristics of each Cycle segment):

- Highest maximum acceleration (at t = 21 s);
- Highest mean acceleration (although speed changes are always of much lower importance for the particular engine owing to the relatively narrow speed range);
- Highest maximum load increase (0–98% at t = 148 s);
- Highest mean load increase; and

- Highest frequency of load increases per minute (this is the most important feature responsible for high emissions following Eqs (4)).

During the second segment of the Cycle the engine experiences the highest mean torque (load), which explains the high values of fuel consumption. On the other hand, the motorway driving (third) part of the ETC Cycle contributes only one sixth of the total soot emissions owing to the smallest average engine torque as well as the fewest abrupt load increases involved.

Things may differentiate when the *normalized* emissions are evaluated, i.e., when the absolute emission values are reduced to the total work produced by the engine during each part of the Cycle, and the emissions (and fuel consumption) are now calculated in g/kWh.

There are two points that require attention in Fig. 7, in comparison to the results presented in Fig. 6: a) the increased amount of NO emissions and fueling during urban driving compared with the rural segment, and b) the relatively high values of both fuel consumption and NO during the motorway driving. Recall from Eq. (5) that in order to normalize the emissions, the total work produced by the engine must first be calculated. Table 2 shows explicitly that the first part of the Cycle is characterized by

- Longest (by far) idling period, typical during this kind of driving; and
- Very long motoring period.

Consequently, work production during urban driving is limited for a considerable part of this segment. As is also obvious in Figs 4 and 5 and quantified in Table 2, the motorway driving part is characterized by relatively low mean engine torque, hence power (since for the current engine the speed range is narrow). Consequently, work production is low here too compared with the rural segment.

The relatively small work produced by the engine during urban and motorway driving compared with the second part of the Cycle, explains the increased amount of normalized NO emissions and fueling in g/kWh. For other engines, however, with broader speed range the differences would not be that dramatic and the reduced emissions and fueling during the motorway driving might be comparable to the ones during the rural segment.

5. Summary, conclusions and future work

An engine mapping-based methodology was developed in order to be able to make a first approximation of engine performance and emissions during a Transient Cycle. The procedure is based on a previous steady-state experimental investigation of the engine for the formulation of polynomial expressions of all interesting engine properties with respect to rotational speed and torque. Correction coefficients are then applied to account for transient discrepancies based on various individual transient events (such as the ones experienced during a Transient Cycle) investigated experimentally and analyzed for the engine under study. The simulation was applied for the case of a heavy-duty diesel engine running on the European Transient Cycle, but can easily be employed to any other torque/speed vs. time transient schedule. It was shown that the most abrupt load increases contribute by far to the total emissions (primarily soot) during the Cycle.

A comparative study was performed for each part of the ETC Cycle, which revealed that for the current engine, the first section (urban driving) is responsible for the biggest amount of emissions (both in g and g/kWh) owing to the most frequent and abrupt load increases and accelerations involved. A comparative analysis was also performed that detailed the individual transient characteristics of each segment of the Cycle.

The obvious advantage of the methodology, apart from its speed and simplicity, is the fact that internal or external (after-treatment) measures effect can then be incorporated in the code/mapping and their contribution to total emissions can be easily quantified. Moreover, various other Cycles can be comparatively studied.

The experimental validation of the proposed methodology as a whole, as well as the extension for the case of vehicular Transient Cycles applying a suitable drivetrain model are under development.

References

[1] http://ec.europa.eu/enterprise/automotive/directives/vehicles/index.htm

[2] http://www.epa.gov/nvfel/testing/dynamometer.htm#engcycles

[3] Winterbone DE. Transient performance. In: Horlock JH, Winterbone DE, editors. The thermodynamics and gas dynamics of internal combustion engines. Vol. II, Oxford: Clarendon Press; 1986.

[4] Watson, N. Eliminating rating effects on turbocharged diesel engine response. SAE Paper 840134; 1984.

[5] Rakopoulos CD, Giakoumis EG. Review of thermodynamic diesel engine simulations under transient operating conditions. SAE Paper 2006-01-0884; 2006. Also, SAE Trans, J Eng 2006;115:467–504.

[6] Rakopoulos CD, Giakoumis EG. Diesel engine transient operation. London: Springer; 2009.

[7] Filipi Z, Wang Y, Assanis D. Effect of variable geometry turbine (VGT) on diesel engine and vehicle system transient response. SAE Paper 2001-01-1247; 2001.

[8] Brahma I, Sharp M, Frazier T. Empirical modeling of transient emissions and transient response for transient optimization. SAE Paper 2009-01-1508; 2009.

[9] Kang H, Farrell PV. Experimental investigation of transient emissions (HC and NOx) in a high speed direct injection (HSDI) diesel engine. SAE Paper 2005-01-3883; 2005.

[10] Krijnsen HC, van Kooten WEJ, Calis HPA, Verbeek RP, van den Bleek CM. Prediction of NOx emissions from a transiently operating diesel engine using an artificial neural network. Chemical Engineering Technol, 1999;22(7):601-7.

[11] Berglund S. A model of turbocharged engines as dynamic drivetrain members. SAE Paper 933050;1993.

[12] Rackmil CI, Blumberg PN, Becker DA, Schuller RR, Garvey DC. A dynamic model of a locomotive diesel engine and electrohydraulic governor. ASME Trans, J Eng Gas Turbines Power 1988;110:405–14.

[13] Directive 1999/96/EC of the European Parliament and of the Council of 13 December 1999.

[14] Celik V, Arcaklioglu E. Performance maps of a diesel engine. Applied Energy 2005;81(3):247-59.

[15] Barelli L, Bidini G, Bonucci F. Development of the regulation mapping of 1 MW internal combustion engine for diagnostic scopes. Applied Energy 2009;86(7-8):1087-1104.

[16] Ericson C, Westerberg B, Egnell R. Transient emission predictions with quasi stationary models. SAE Paper 2005-01-3852, 2005.

Figures Captions

1. The European Transient Cycle (ETC) for heavy-duty engines.
2. Block diagram of applied methodology.
3. Results of current engine mapping over the whole operating range for NO, soot and fueling, including detailed soot and NO values for engine operation at 1000 rpm.
4. Calculated performance results during the ETC Transient Cycle.
5. Calculated emission results during the ETC Transient Cycle.
6. Calculated contribution of each segment of the ETC Cycle on the total NO, soot and fuel consumption.
7. Calculated comparative emissions and fueling between the three segments of the Cycle (g/kWh).

Figure 1

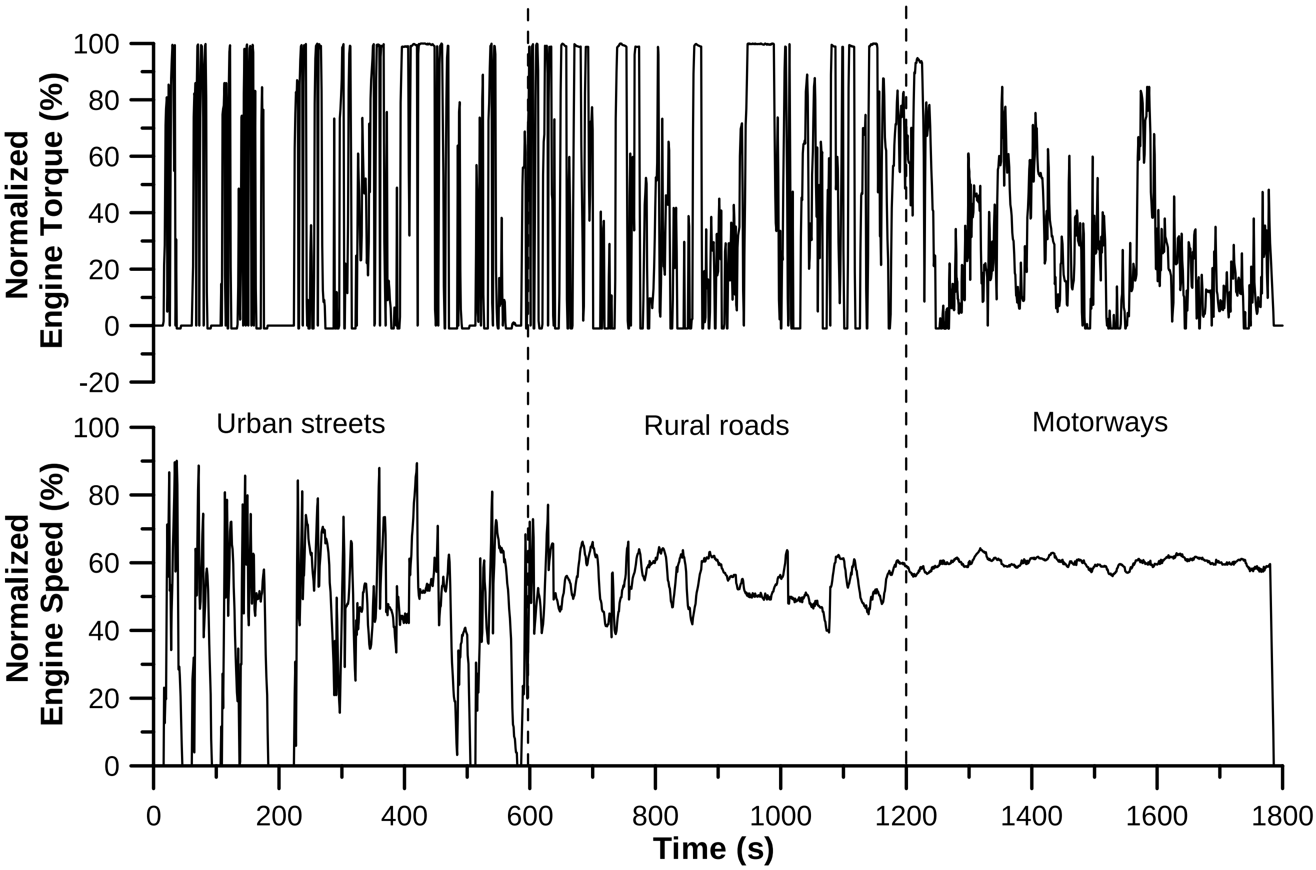

Normalized Engine Torque (%)
100
80
60
40
20
0
-20
Normalized Engine Speed (%)
100
80
60
40
20
0
Urban streets
Rural roads
Motorways
0
200
400
600
800
1000
1200
1400
1600
1800
Time (s)

Figure 2

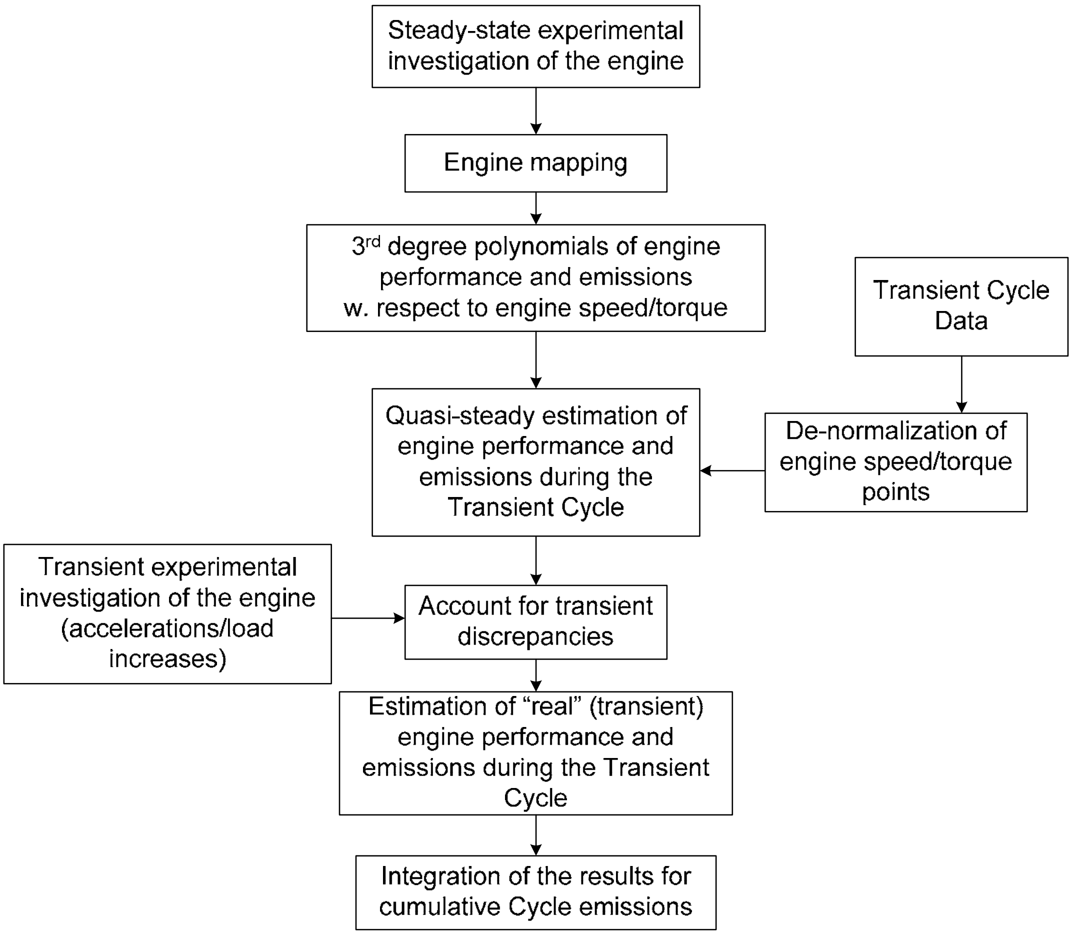

Steady-state experimental investigation of the engine
Engine mapping
3rd degree polynomials of engine performance and emissions w. respect to engine speed/torque
Transient Cycle Data
Quasi-steady estimation of engine performance and emissions during the Transient Cycle
De-normalization of engine speed/torque points
Transient experimental investigation of the engine (accelerations/load increases)
Account for transient discrepancies
Estimation of “real” (transient) engine performance and emissions during the Transient Cycle
Integration of the results for cumulative Cycle emissions

Figure 3

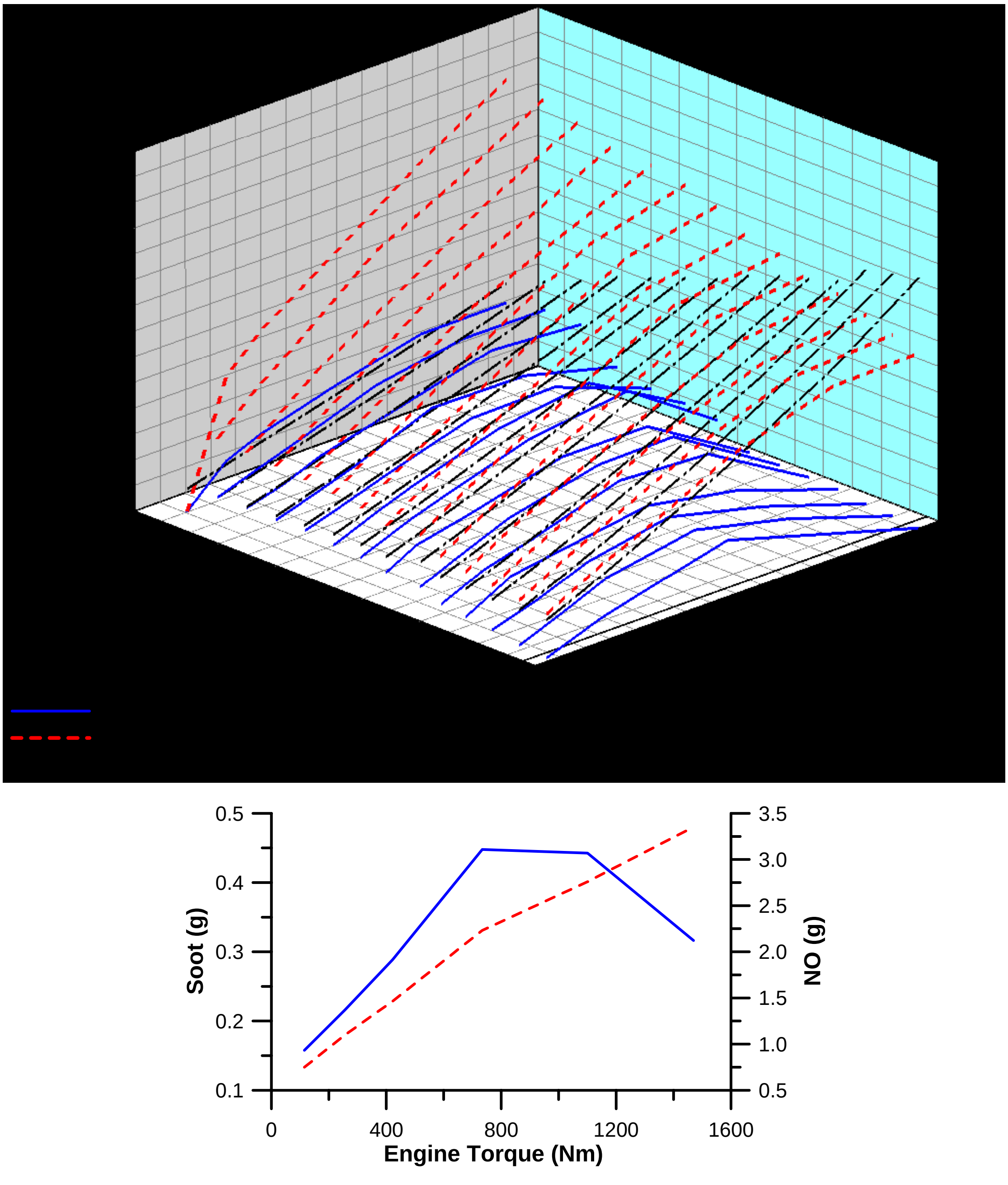

0.5
0.4
0.3
0.2
0.1
Soot (g)
3.5
3.0
2.5
2.0
1.5
1.0
0.5
NO (g)
0
400
800
1200
1600
Engine Torque (Nm)

Figure 4

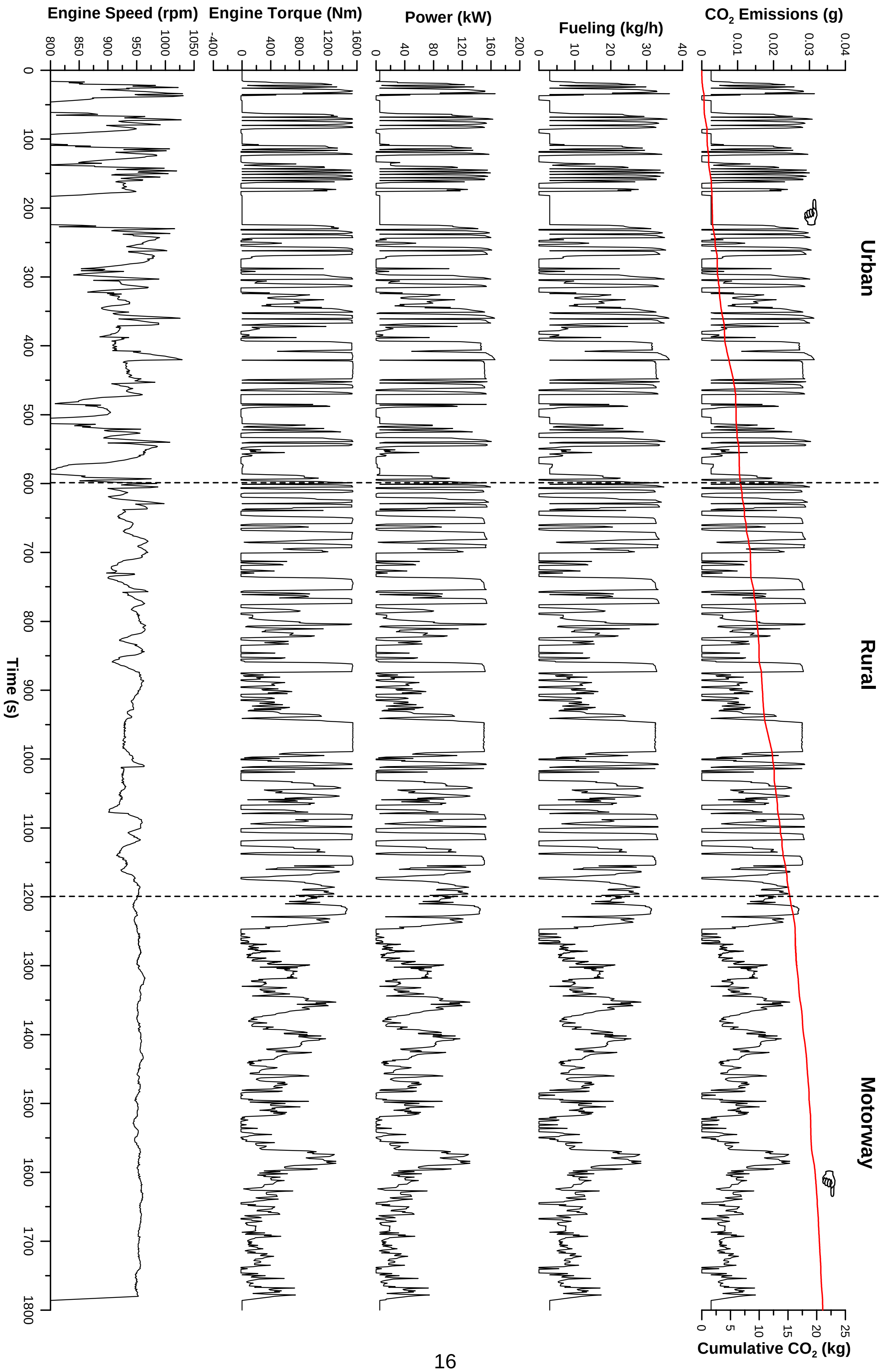

Urban
Rural
Motorway
CO_2 Emissions (g)
Fueling (kg/h)
Power (kW)
Engine Torque (Nm)
Engine Speed (rpm)
Time (s)
Cumulative CO_2 (kg)

Figure 5

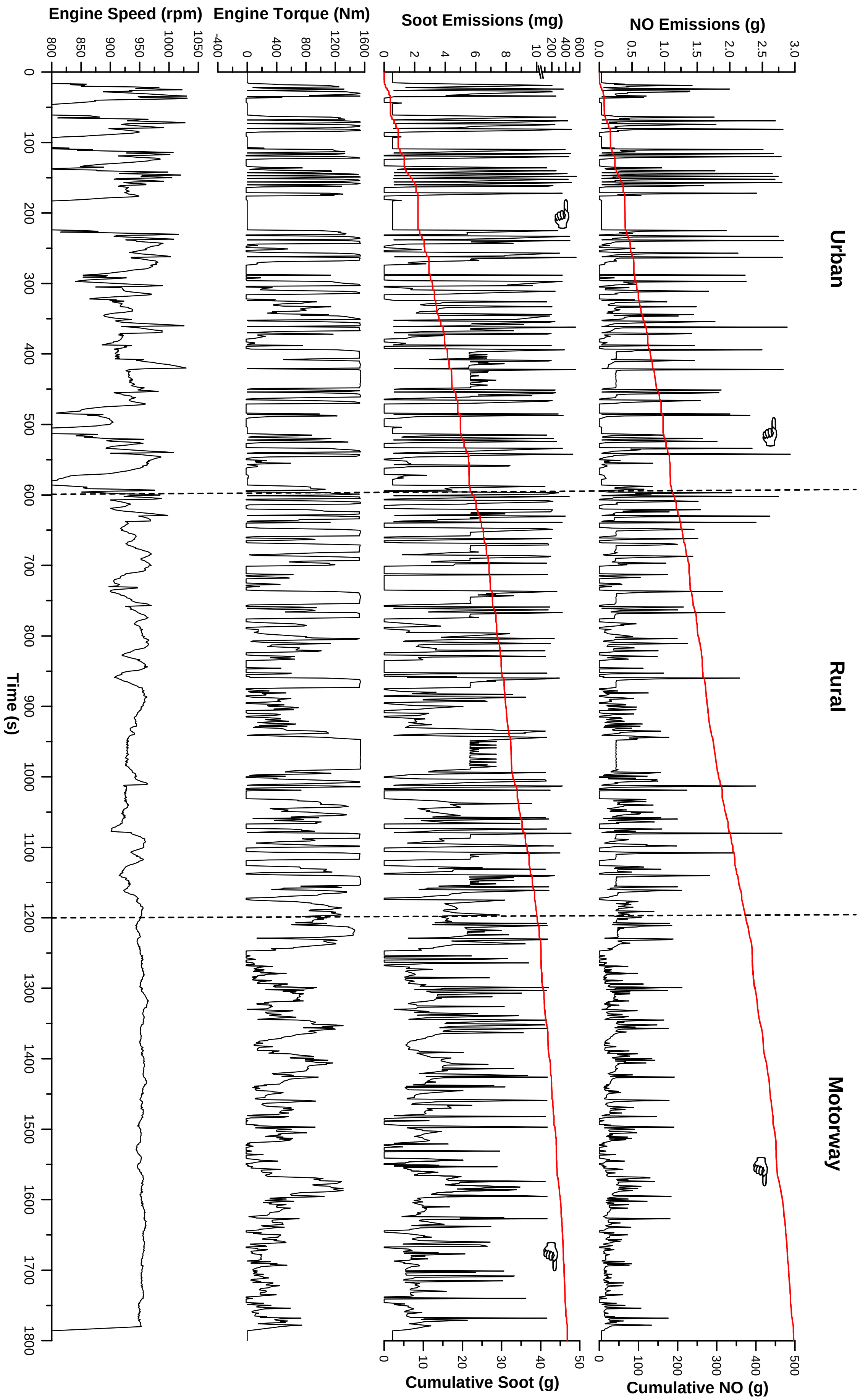

NO Emissions (g)
Soot Emissions (mg)
Engine Torque (Nm)
Engine Speed (rpm)
Time (s)
Cumulative Soot (g)
Cumulative NO (g)
Urban
Rural
Motorway

Figure 6

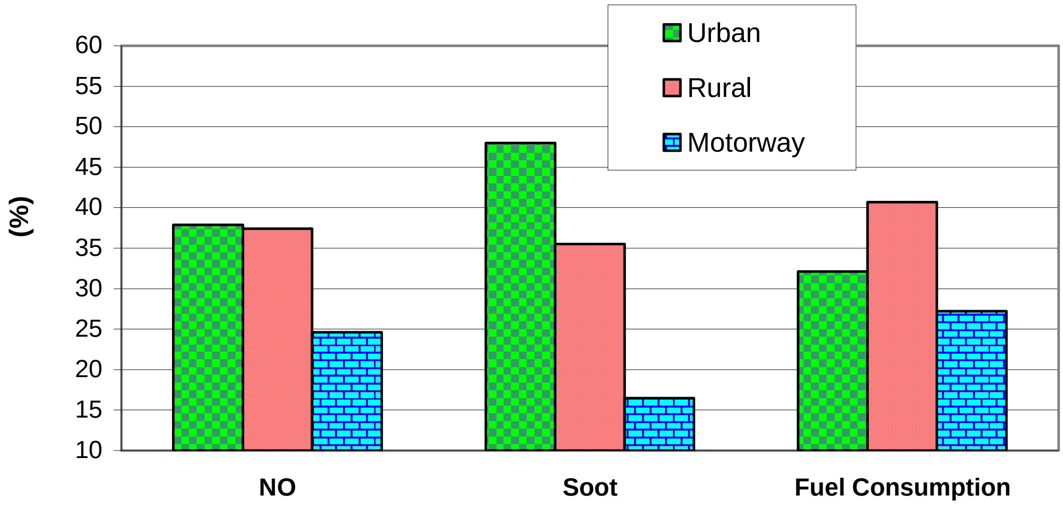

Figure 7

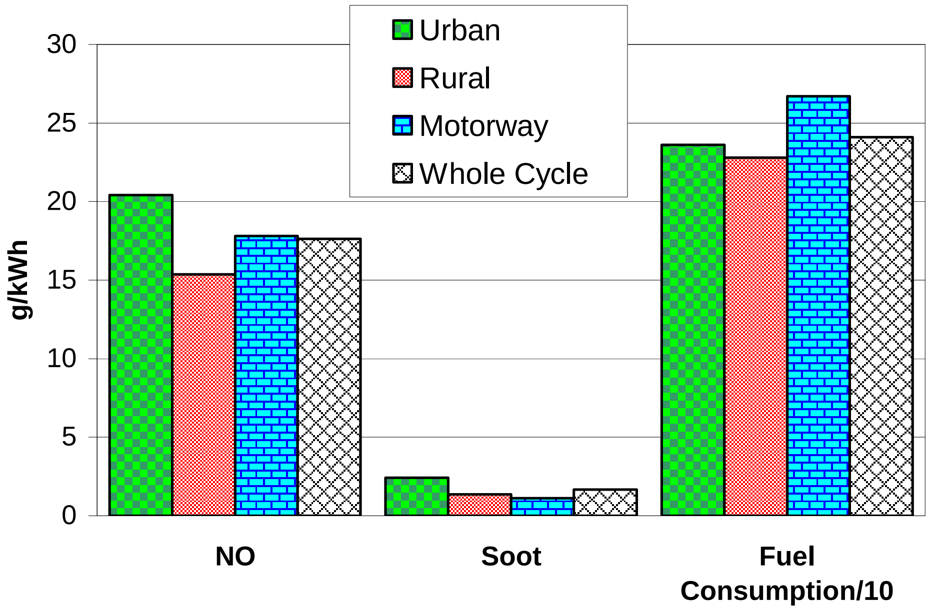

Table 1. Data of the engine used for the analysis

Engine Type	In-line, six-cylinder, four-stroke, turbocharged heavy-duty diesel engine
Speed Range	800–1500 rpm
Bore / Stroke	140 mm / 180 mm
Compression Ratio	17.7:1
Maximum Power	320 HP (236kW) @ 1500 rpm
Maximum Torque	1520 Nm @ 1250 rpm

Table 2. Comparison of the individual characteristics of the three parts of the ETC Transient Cycle

	Duration (s)	Average (normalized) speed (%)	Maximum (normalized) speed (%)	Average torque (%)	Maximum torque (%)	Idling period (%)	Motoring period (%)
1st part (urban)	600	40.31	90.1	35.57	100	23.17	22.33
2nd part (rural)	600	54.17	77.1	47.44	100	1.33	22.50
3rd part (motorway)	600	58.12	64.3	26.47	94.8	3.50	9.17
Whole Cycle	1800	50.86	90.1	36.50	100	9.33	18.0

Table 3. Comparison of the individual transient characteristics of the three parts of the ETC Transient Cycle

	Number of torque reversals (min^{-1})*	Maximum acceleration for current engine (%)	Mean normalized acceleration (%)	Maximum load increase	Mean load increase (%)	Number of greater than 300% / 500% / 1000% load increases (min^{-1})
1st part (urban)	1.50	10.52 @ t = 21 s	7.30 (24.2 per min)**	0–98% @ t = 148 s	22.62 (19.7 per min)**	5.90 / 5.50 / 5.10
2nd part (rural)	2.40	5.35 @ t = 731 s	1.39 (29.4 per min)**	0–88.9% @ t = 1080 s	15.72 (23.0 per min)**	4.80 / 4.10 / 3.70
3rd part (motorway)	0.70	0.42 @ t = 1472 s	0.61 (25.5 per min)**	0–36.2% @ t = 1482 s	9.15 (22.1 per min)**	2.90 / 1.80 / 1.10
Whole Cycle	1.53	10.52 @ t = 21 s	2.81 (26.3 per min)**	0–98% @ t = 148 s	15.51 (21.7 per min)**	4.53 / 3.80 / 3.30

* from motoring to at least 5% positive torque within one second

** number of increases